Estimation of Refraction Index for Color Image Rendering

Norihiro Tanaka and Shoji Tominaga
Osaka Electro-Communication University
Department of Engineering Informatics
Neyagawa, Osaka, Japan

Abstract

The present paper describes a method for estimating the refraction index of the material of an object surface with arbitrary convex shape in natural scenes. The refraction index cannot be neglected for describing the specular reflection function, while the absorption index can be neglected for the dielectric material. In fact, note that the intensity of specular highlight depends greatly upon the index refraction of the surface material. In this paper, we consider estimating the refraction index for any object surfaces of inhomogeneous dielectric materials in natural scenes by using a general CCD camera. This parameter is estimated from the sensor measurements for specular highlight intensity of an object surface at different conditions of illumination and viewing. The estimated refraction index is compared with direct measurements using a refractmeter. The accomplishment of this estimation leads us to complete estimation of various parameters of the Torrance-Sparrow model.

Introduction

Knowing reflection properties of the material of which an object surface is made is very important for color image rendering in computer graphics. The reflection properties of an object surface are modeled using optical parameters of the surface material. The principal parameters needed for modeling the surface reflection are surface-spectral reflectance, surface roughness, index of refraction, absorption index, and reflection intensity. A three-dimensional (3D) reflection model is described using such parameters. The authors have been working on estimation of various parameters of a reflection model from image data of an object taken by a CCD camera. In a previous paper[1] we used the Phong model as a reflection model to estimate the surface-spectral reflectance and surface roughness. However this model was too simple to produce realistic images. In fact the Phong model has difficulty in describing the specular reflection because the Fresnel term is neglected. Other works on reflection modeling are found in Refs. 2 and 3. They used gonio-metric methods and also neglected the Fresnel term. The Fresnel term cannot be neglected for realistic rendering of glossy and specular surfaces. We extended the previous parameter estimation technique to the Torrance-Sparrow model.[4] The specular reflection function is described in terms of the distribution of isotopic orientation, the geometrical attenuation factor, and the Fresnel term. If we assume that an object surface is made of inhomogeneous dielectric material, most parameters of the Torrance-Sparrow model, except for the index of refraction, can be estimated from a single image by a calibrated CCD camera.

The present paper describes a method for estimating the refraction index of the material of an object surface with arbitrary convex shape in natural scenes. The refraction index cannot be neglected for describing the specular reflection function, while the absorption index can be neglected for the dielectric material. In fact, note that the intensity of specular highlight depends greatly upon the index refraction of the surface material. Recently Obein et al.[5] proposed a measurement method for knowing the value of the refraction index of a plane sample. They developed a special equipment based on combination of Fourier optics and a cooled CCD sensor. In this paper, we consider estimating the refraction index for any object surfaces of inhomogeneous dielectric materials in natural scenes by using a general CCD camera. This parameter is estimated from the sensor measurements for highlight peaks of an object surface at different conditions of illumination and viewing. The estimated refraction index is compared with direct measurements using a refractmeter.

The accomplishment of this estimation leads us to complete estimation of various parameters of the Torrance-Sparrow model, such as (1) spectral reflectance, (2) illuminant spectrum, (3) surface roughness, (4) ratio of body to interface intensity, and (5) index of refraction. The overall feasibility of our method is confirmed based on computer graphics images created by using the estimated parameters.

Measurement System

Figure 1 shows the scene for measuring reflection properties of an object surface. The apparatus consists of a lighting system, a goniometric rotating table, and a vision system. Figure 2 depicts the schematic diagram of the measuring system. The lighting system emits parallel beams from a tungsten halogen lamp. An object sample is mounted on the turn table about which a 70 cm arm is able to rotate. At the end of the arm is a multiband camera for spectral imaging. The object sample can be rotated independent of the arm so that all incident/viewing angle configurations can be created for in-plane reflection. The condition that the emitted rays are parallel beams is crucial for reliable measurement of the object surface. The emitted rays are quite uniform in a region of 70mm x 70mm at the location of the turn table. Figure 3 shows a geometric model for measuring a specular highlight on a curved surface. The index of refraction is estimated from the highlight measurements with different light angles.

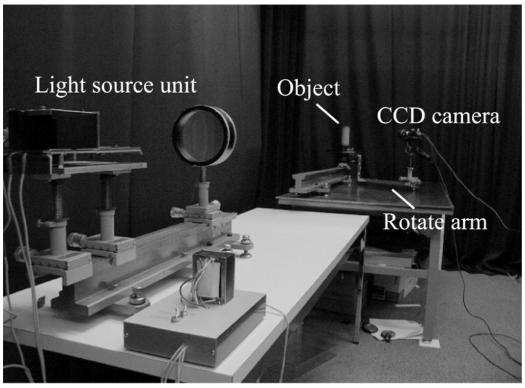

Figure 1. Measurement scene.

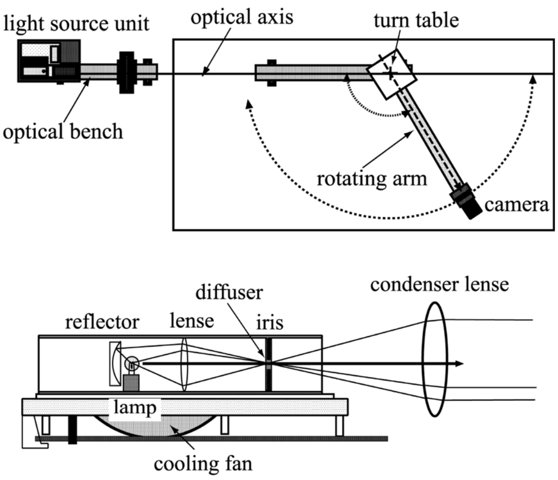

Figure 2. Schematic diagram of the measuring system

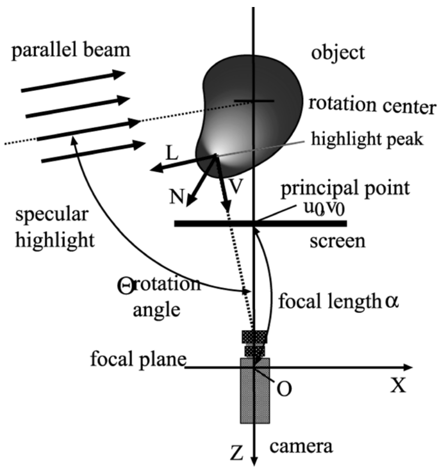

Figure 3. Model for measuring a specular highlight.

Reflection Model

The spectral radiance distribution $Y(x,\lambda)$ from a reflective object surface is a function of the spatial location x and the wavelength λ. The Torrance-Sparrow model is described as

$$Y(x,\lambda) = \alpha \cos(\theta_i) S(\lambda) E(\lambda) + \beta \frac{D(\varphi) G(\mathbf{N},\mathbf{V},\mathbf{L}) F(\theta_Q, n)}{\cos(\theta_r)} E(\lambda), \qquad (1)$$

where the first and second terms represent, respectively, the diffuse and specular reflection components. $S(\lambda)$: spectral reflectance, $E(\lambda)$: illuminant spectral distribution, θ_i: angle of incidence, θ_r: viewing angle, φ: angle between global surface normal and micro-facet normal, θ_Q: angle of incidence to micro-facet. The interface reflection component consists of several terms, D: function providing the index of surface roughness defined as $\exp\{-\ln(2)\varphi^2/\gamma^2\}$, where the .γ is constant. G: geometrical attenuation factor, and F: Fresnel spectral reflectance, where n is the index of refraction.

We performed a simulation experiment for suggesting how important the index of refraction n is in rendering realistic image. Figure 4 shows the directional reflectance distribution with different values of the refraction index n in the Torrance-Sparrow model, where the other parameters are set to $S(\lambda) = 1$, $E(\lambda) = const$, $\alpha = 1.0$, $\beta = 6.0$, and $\gamma = 0.08$ *radian*. It is noted that specular highlight is affected by the refraction index and the magnitude increases with the refraction index value.

Figure 5 shows a set of computer graphics images of yellow plastic cylinders. We used the measured spectral reflectance of a real plastics object for $S(\lambda)$ and the measured spectral distribution of an incandescent lamp for $\alpha = 1.0$, $\beta = 6.0$, and $\gamma = 0.08$ *radian.* Note that the appearance of specular highlights on cylinder surfaces changes greatly with the refraction index.

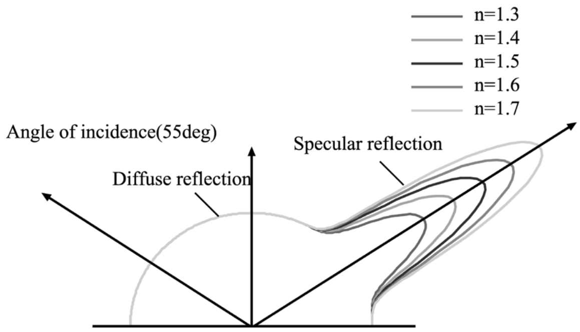

Figure 4. Directional reflectance distribution with different values of the refraction index.

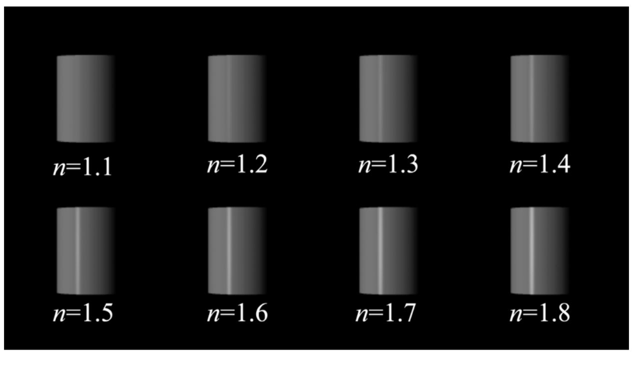

Figure 5. CG image of yellow plastic cylinders with different values of the refraction index.

Estimation Algorithm

1. Histogram Analysis

The multiband camera system consists of six color sensors. The camera outputs are described as

$$\rho_k(x) = \int Y(x,\lambda) R_k(\lambda) d\lambda, (k = 1,2,...,6) \quad (2)$$

where $R_k(\lambda)$ is the spectral sensitivity functions of the sensor k. From the dichromatic reflection property of Eq. (1), the sensor output vector $\rho(=[\rho_1, \rho_2, \ldots, \rho_6]^t)$ for any spatial location on an object is expressed in a linear combination of the two reflection component of body and interface as

$$\rho = \rho_B + \rho_I = w_B \mathbf{c}_B + w_I \mathbf{c}_I. \quad (3)$$

These two vectors span a two-dimensional subspace (plane) in the six-dimensional sensor space, and all the camera outputs observed from the same object surface fall in this subspace.

The pixel distribution (histogram) in the sensor space consists of two linear clusters of pixels: the matte cluster by body reflection and the highlight cluster by interface reflection. Therefore the histogram can be projected onto the subspace spanned by the two component vectors. From the image data, this subspace is determined by finding two principal components of the sensor output data. Figure 6 show a sketch of the histogram on the subspace (*u, v*), where the linear cluster of body reflection coincides with the *u*-axis. The point P_b indicates an extreme point on the linear body cluster, corresponding to the maximal body reflection component. The point H_m indicates a peak point on the specular highlight cluster. From the image data, this point is determined as a point with a maximum *v* value.

The specular highlight peak on an observed object surface has the maximal specular reflection component. At the peak, the distribution function D takes the maximum as D = 1 since $\varphi = 0$. The sensor output ρ_I for this maximal interface component, except for the body component, is expressed in the form

$$\rho_I = \beta \frac{F(\theta_Q, n)}{\cos(\theta_r)} \int E(\lambda) \begin{bmatrix} R_1(\lambda) \\ R_2(\lambda) \\ \vdots \\ R_6(\lambda) \end{bmatrix} d\lambda. \quad (4)$$

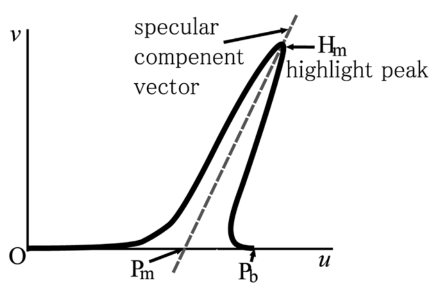

Figure 6. Histogram on the subspace.

2. Computation of Viewing and Incident Angles

We estimate the refractive index *n* from the specular reflection at the mirror angle $\varphi = 0$. We need the viewing angle θ_r and light incident angel θ_i at the mirror reflection point. When we assume the parallel light beams, the light vector **L** is described with the rotation angle as **L** = [cos Θ, 0, - sin Θ]. The viewing vector at location (x, y) on the image plane is described with the camera parameters as **V** = $[x - v_0, y - u_0, \alpha]$ This directional vector is normalized as |**V**| = 1. Then the angles θ_r and θ_i are obtained from the geometric relationship among **L**, **V**, and **N.**

3. Specular Intensity Fitting

The specular intensity at the mirror reflection point depends on the refractive index *n*, the incident angle θ_i, and the constant coefficient β. Note that it is independent of roughness γ. Therefore the problem of estimating the refractive index *n* can be solved as the fitting problem of highlight peak. That is, the model function with unknown *n* is fitted to the intensity data of mirror reflection acquired at different angles of θ_i. The criterion function for this fitting is described as

$$f = \sum_{\theta_i} \left(\| \rho_I(\theta_i) \| - \beta \frac{F(n, \theta_i)}{\cos\theta_i} \right)^2, \quad (5)$$

where $\|\rho_I(\theta_i)\|$ is the intensity of mirror reflection at θ_i. This intensity value is obtained from the histogram analysis of the image pixels, which depends on object shape. The parameters *n* and β minimizing the function are solved as a least-squared solution of the nonlinear fitting problem. We use the Levenberg-Marquardt method for this solution.

4. Refractive Index in Two Cases

Cylindrical Object:

It should be noted that the highlight peak for a rough surface is not always coincident with the mirror reflection satisfying $\theta_i = \theta_r = \theta_Q$. The specular peak, appearing at a point shifted from the mirror reflection point, is called the off-specular peak. If the surface shape is known as a cylinder, we can estimate the surface normal at any point on the cylinder from the calibrated image data. Therefore we can easily find the (x, y) coordinate point satisfying $\theta_i = \theta_r$. The above specular intensity fitting is done at this point for estimating the refractive index of the material.

Object With General Shapes:

It is not easy to estimate the surface normal for an object with general shape. Therefore we assume that highlight peak appears at the mirror reflection point. This assumption is valid for smooth surface. The surface normal at the specular highlight peak is calculated as **N = (L + V) / |L + V|**. Then θ_r and θ_i are obtained with $\theta_i = \theta_r$.

Experimental Results

First, we estimate the refraction index of a cylinder surface. Figure 7 shows a set of color images of an orange painted cylinder at different light incident angles. These images were observed at the incident angles, spanning 16 degrees to 61 degrees in 2.5 degree increments. The specular intensity fitting at the mirror reflection points provided the estimated value n = 1.44 for the refraction index. The direct measurement by the Abbe refractmeter provided n = 1.45. Figure 8 depicts the fitting results of the specular function at the mirror reflection points, where a set of three curves compares among specular intensities in camera data, intensities by the model function using the estimated refraction index, and intensities by the model function using the measured refraction index. We can see in Figure 8 that the estimate provides an accurate fit to the mirror specular intensities at different incident angles.

Next, we estimate the index of an object with general shape. Figure 9 shows a set of observed images of an orange painted dish at the incident angles of 16 to 61 degrees in 2.5 degree increments. Figure 10 depicts the fitting results of the specular function at highlight peaks. The best fitting is obtained at n = 1.52. Again the estimate provides a good fit at different incident angles. Figure 11 shows the computer graphics image of the painted object for the incident angle θ_i = 36 degrees. The image was created using all the estimated parameters of $S(\lambda)$, $E(\lambda)$, α = 78.3, β = 397.5, and γ = 0.13 *radian*. The spatial coordinates of the object were measured by a laser range finder and the object surface was represented by triangular meshes. A ray tracing algorithm was used for rendering the realistic 3D image under arbitrary conditions of illumination and viewing. A comparison between the measured image and the CG image suggests a reliability of the proposed method.

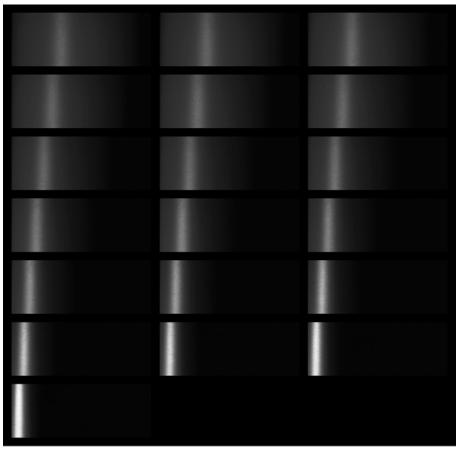

Figure 7. Set of observed images of an orange painted cylinder at different light incident angles

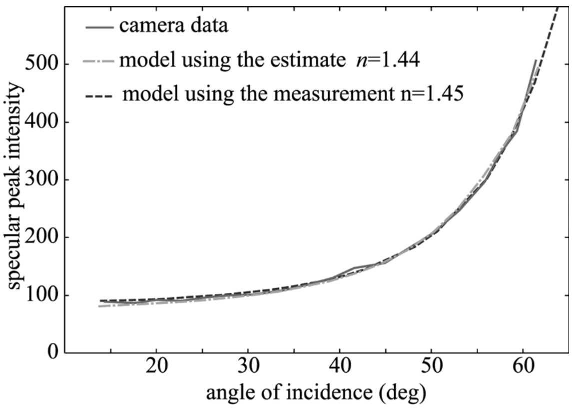

Figure 8. Fitting results of specular peaks for the cylinder images.

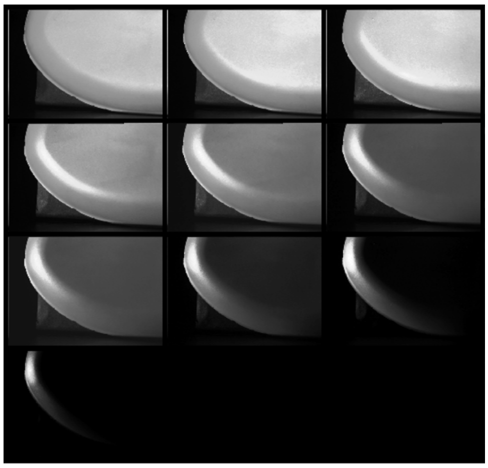

Figure 9. Set of observed images of an orange painted dish at different light incident angles.

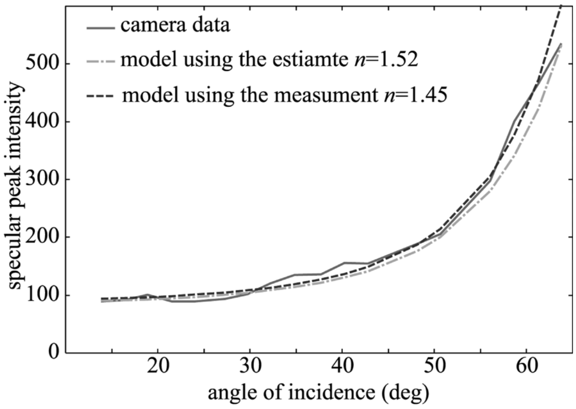

Figure 10. Fitting results of specular peaks for the dish image.

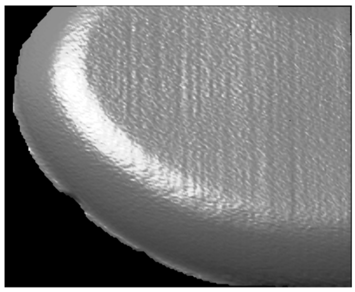

Figure 11. CG image rendered with all the estimated parameters at incident angle of 36 degrees.

Conclusion

This paper has described a method for estimating the refraction index of the material of an object surface with arbitrary convex shape. We supposed that the surface was composed of an inhomogeneous dielectric material like paint or plastic. A lighting system emitting parallel beams and a multiband CCD camera were used for measuring various reflection parameters. The refraction index parameter was estimated from the sensor measurements of specular intensities at the mirror reflection points when the illumination and viewing angles changed. The estimated refraction index was compared with direct measurements using a refractmeter. The overall feasibility of our method was confirmed based on computer graphics images created by using the estimated parameters of various reflection parameters in the Torrance-Sparrow model.

Reference

1. S. Tominaga and N. Tanaka: a Estimation of reflection parameters from a single color image *IEEE Computer Graphics and Applications*, Vol.20, No.5, pp.58-66 (2000).
2. Y. Sato, M.D. Wheeler, and K. Ikeuchi: Object shape and reflectance modeling form observation, SIGGRAPH 97, pp. 379-387 (1997)
3. H. Haneishi, T. Iwanami, N. Tamura, and Y. Miyake: Goniospectral Imaging of 3D object, *Proc. of the IS&T/SID Color Imaging Conference*, pp.173-176, (1998).
4. N. Tanaka and S. Tominaga: Measurement of surface reflection properties, *Proc. of IS&T/SID's 9th Color Imaging Conference*, pp.52-55, (2001) .
5. G. Obein, T. Leroux, and F. Vienot: Bi-directional reflectance distribution factor and gloss scales, *Proc. of SPIE, Human Vision and Electronic Imaging VI*, Vol. 4299, pp. 279-290 (2001).

Biography

Norihiro Tanaka is a visiting researcher in Osaka Electro-Communication University, Neyagawa, Osaka, Japan. His research interests include reflection modeling and its application to computer graphics and computer vision. He received the B.E. ,M.E. and Ph.D degrees in computer science from Osaka Electro-Communication University in 1995, 1997 and 2001, respectively.

Shoji Tominaga is a Professor in the Department of Engineering Informatics at Osaka Electro-Communication University, Neyagawa, Osaka, Japan. His research interests include computational color vision, color image analysis, reflection modeling, and computer graphics. He received the B.E., M.S., and Ph.D. degrees in electrical engineering from Osaka University, Toyonaka, Osaka, Japan, in 1970, 1972, and 1975, respectively. He is a member of IEEE, Optical Society of America, ACM.